



Intercalibration of Vegetation Indices from Landsat ETM+ and MODIS 500m Data for LAI mapping

N. Rochdi and R. Fernandes

2008

Geomatics Canada

Technical Note 3



©Her Majesty the Queen in Right of Canada 2008

ISSN 1914-4229

Catalogue No. M103-1/3-2008E-PDF

ISBN 978-1-100-10895-7

A copy of this publication is also available for reference in depository libraries across Canada through access to the Depository Services Program's Web site at <http://dsp-psd.pwgsc.gc.ca>

A free digital download of this publication is available from GeoPub:
http://geopub.nrcan.gc.ca/index_e.php

Toll-free (Canada and U.S.A.): 1-888-252-4301

Recommended citation

Rochdi N., and Fernandes R., 2008. Intercalibration of Vegetation Indices from Landsat ETM+ and MODIS 500m Data for LAI mapping; Geomatics Canada, Technical Note 3, 11 p.

Critical reviewers

Gunar Fedosejevs

Abdelgadir Abuelgasim

Authors

N. Rochdi

R. Fernandes (rfernand@nrcan.gc.ca)

Canada Centre for Remote Sensing

Natural Resources Canada

Ottawa, ON K1A 0Y7

Correction date:

**All requests for permission to reproduce this work, in whole or in part, for purposes of commercial use, resale, or redistribution shall be addressed to: Earth Sciences Sector Copyright Information Officer, Room 644B, 615 Booth Street, Ottawa, Ontario K1A 0E9.
E-mail: ESSCopyright@NRCan.gc.ca**

Intercalibration of Vegetation Indices from Landsat ETM+ and MODIS 500m Data for LAI mapping

N. Rochdi and R. Fernandes

Rochdi N., and Fernandes R., 2008. Intercalibration of Vegetation Indices from Landsat ETM+ and MODIS 500m Data for LAI mapping; Geomatics Canada, Technical Note 3, 11p.

Abstract: This paper develops and applies a direct approach to vegetation index (VI) intercalibration between sensors of different spatial resolutions that have near-simultaneous acquisitions, similar spectral bands, and similar acquisition geometry. Vegetation indices (VIs) that have shown good performances to map leaf area index (LAI) methods such as simple ratio (SR), infrared simple ratio (ISR), and reduced simple ratio (RSR) were investigated together with the normalized difference vegetation index (NDVI). This study is specifically dedicated to the intercalibration of TERRA/MODIS and LANDSAT 7/ETM+ sensors.

Résumé : Nous exposons dans ce document l'élaboration et l'application d'une méthode directe pour l'interétalonnage des indices de végétation au moyen de capteurs de différentes résolutions spatiales permettant l'acquisition quasi simultanée dans des bandes spectrales similaires et présentant des géométries d'acquisition similaires. Les indices de végétation qui ont donné de bons résultats pour la cartographie de l'indice de surface foliaire, notamment le rapport simple, le rapport simple dans l'infrarouge et le rapport simple réduit, ont fait l'objet d'un examen, de même que l'indice de végétation par différence normalisée. Cette étude porte particulièrement sur l'interétalonnage des capteurs TERRA/MODIS et LANDSAT7/ETM+.

INTRODUCTION AND OBJECTIVES

Spectral vegetation indices (VIs) derived, in general, from nonlinear combinations of shortwave radiances, are widely used for monitoring vegetation both in situ using radiometers and remotely via satellite or airborne imaging sensors. Vegetation indices have been used to estimate biophysical parameters such as leaf area index (LAI), biomass, tree canopy cover, vegetation moisture status, and vegetation chlorophyll content. Vegetation indices have also found application in monitoring growing season length, terrestrial carbon sinks, photosynthetic function, and crop evapotranspiration. In all of these applications the VIs were designed to suppress ‘noise’ due to environmental factors such as atmospheric effects or background reflectances, while preserving sensitivity to vegetation properties.

There have been a number of investigations to intercalibrate vegetation indices across sensors based on model simulations or measurements for different Earth observation satellites (Venturini et al., 2004; Miura et al., 2006). Using hyperspectral data from the HyMap sensor over tropical savanna, Galvao et al. (1999) pointed out that sensitivity of the normalized difference vegetation index (NDVI) to spectral band specifications may be significantly lower if the surface-reflectance spectrum is relatively constant across the corresponding bands of the sensors being intercalibrated. Teillet et al. (2006) provided, based on airborne and ground measurements data, a cross-comparison of four ‘fine-resolution’ satellite sensors (Landsat 5 Thematic Mapper, Systeme Pour Observation Terrestre (SPOT) – 5 HRG, Indian Remote Sensing (IRS)-P6 LISS-III, Chinese Brazilian Environmental Remote Sensing (CBERS)-2 High Resolution Charge Coupled Device (HRCC)) to Landsat 7 Enhanced Thematic Mapper Plus (ETM+) using spectral simulations of the simple ratio (SR), soil adjusted vegetation index (SAVI), global environmental monitoring index (GEMI), soil adjusted and atmospherically resistant vegetation index (SARVI), atmospherically resistant vegetation index (ARVI), MODIS enhanced vegetation index (MEVI), and modified triangular vegetation index 2 (MTVI2) indices. They reported that over the four distinct surface targets investigated (boreal forest, rangeland, grassland, and bright vegetation), relative differences ranging from 0.5% to 22% were possible due to spectral differences between sensors.

Direct comparisons of VIs derived from sensor measurements offer an alternate approach to intercalibration. Brown et al. (2006) performed an empirical comparison of sixteen-day composite NDVI values observed with moderate-resolution MODIS on TERRA (MODIS) and NOAA-16 AVHRR, stratified by land cover, to demonstrate that relatively consistent linear VI intercalibrations are possible.

There are two areas where spectral intercalibration studies have not been as common. The first being between sensors having either coincident or almost coincident overpasses on the same orbital tracks. More importantly there has been

little work on the intercalibration of moderate- and fine-resolution sensors that have similar acquisition characteristics. Liang et al. (2002) relied on the pairs of TERRA/MODIS and Landsat ETM+ acquisitions to evaluate reflectance and albedo retrievals, but did not go so far as intercalibrating VIs. A second gap in the literature is related to the lack of VI intercalibration studies that include VIs derived from shortwave infrared (SWIR) bands. Such VIs could substantially reduce sensitivity to atmospheric effects (Kauffman and Tanré, 1992). There is increasing evidence that these indices may also be more appropriate, in comparison to indices using only visible and near infrared (NIR) bands, for certain applications (Nemani et al., 1993; Gao et al., 2000; Fernandes et al., 2003).

Objective

In this paper, we focus on a specific goal of intercalibrating VIs between sensors of different spatial resolutions that have near-simultaneous acquisitions, similar spectral bands, and similar acquisition geometry. The scope of our study is further narrowed to deal with VIs that have demonstrated relationships to in situ LAI — the SR, RSR, and ISR methods (Galvao et al., 1999; Fernandes et al., 2003).

Our emphasis on LAI is twofold. Firstly, recent comparison studies suggest that locally calibrated regressions between VIs and LAI are capable of meeting Global Climate Observing System targets for accuracy in contrast to globally parameterized radiative transfer models (Abuelgasim et al., 2006; Garrigues et al., 2006). Secondly, by cross-calibrating VIs it is also possible to use fine-resolution scenes to explain anomalies in moderate-resolution time series over mixed targets. The investigations carried out in this paper aims to address the following three objectives:

1. intercalibration of RED, NIR, SWIR bands and vegetation indices from ETM+ and MODIS 500 m,
2. evaluation of the land cover and regional effect on sensor intercalibration, and
3. assessment of the 500 MODIS LAI derived based on the VI intercalibration.

METHOD

We performed intercalibration within two global biomes (boreal and northern temperate forests) and across two different ecological zones within each biome.

In order to constrain the intercalibration process, the same acquisition date for both ETM+ and MODIS sensors was used at each study area so that their overpass times were never greater than 40 minutes apart. This implies less than 4.5 degrees difference in illumination angle between sensors for each location. View-angle differences between sensors

are negligible, corresponding essentially to the angle subtended by half a MODIS pixel within the ± 7 degree range of nadir corresponding to an ETM+ swath, since they follow the same orbit and are both whiskbroom scanners.

Study area

The study areas were located in four sites selected from four different ecological zones (ecozones) in Canada. Each area belongs to a specific ecozone characterized by a predominant physical habitat type and species assemblage. The four sites used were:

- Atlantic maritime (AM) study area located in central Nova Scotia (centred at 44.60° N and 64.25° W) in the Atlantic maritime ecozone within the northern temperate forest biome.
- mixed wood plains (MWP) study area centred at 45.29° N and 76.37° W and located in the mixed wood plains ecozone within the northern temperate forest biome.
- boreal shield (BS) study area centred at 88.91° W and 48.86° N and part of the boreal shield ecozone.,
- taiga shield (TS) study area centred at 75.56° W and 54.52° N and located in the Taiga Shield ecozone.

Landsat data preprocessing

Georeferenced Landsat 7 ETM+ level L1G at-sensor-radiance scene covering each study area (Table1) were selected to correspond to mid-growing season, relatively cloud-free conditions, although some clouds and haze were included to capture typical acquisition conditions of data used in operational mapping applications. Digital counts were converted to at-sensor radiance using time-dependent calibration coefficients provided online using the method specified in the Landsat-7 Science Data User's Handbook, (USGS, 2004).

Aerosol optical depth at 550 nm (AOD550), and water vapour and ozone concentrations were taken from the MODIS/terra atmosphere products MOD04 (version 4), MOD05 (version 4), and MOD07 (version 5) ([http://modis-atmos.gsfc.](http://modis-atmos.gsfc.nasa.gov/products.html)

[nasa.gov/products.html](http://modis-atmos.gsfc.nasa.gov/products.html)) corresponding to the Landsat overpass. Reprojection and subsetting of the MODIS atmosphere swath product was performed using the reprojection tool developed by Khlopenkov et al. (2006) to avoid additional spatial-registration errors by directly using geolocation fields for reprojection.

Atmospheric correction was applied to the ETM+ scenes using the 6S model version 4.1 (Vermote et al., 1997). The ETM+ scenes were projected from Universal Transverse Mercator (UTM) to Lambert Conformal Conic (LCC, with 95°W as the reference meridian, 49°N and 77°W as standard parallels) using a nearest neighbour resampling algorithm.

Land-cover maps, at 30 m resolution, corresponding to the four ETM+ scenes were obtained from the Satellite Information for Land Cover of Canada (SILC) database (Baubien et al., 2002). The classification legend follows the Federal Geographic Data Committee (FGDC) National Vegetation Geographic System (NVGS) nomenclature composed of 44 land-cover classes (Table 2) (Cihlar et al., 2003).

MODIS data preprocessing

MODIS/Terra surface reflectance daily L2G Global 500 m SIN Grid product, MOD09GHK (collection 4) (<http://modis-land.gsfc.nasa.gov/surfrad.htm>) and MODIS/Terra top-of-atmosphere radiance daily L1B 500m swath product MOD02HKM (collection 5) were used in this study. Independent intercalibration of ETM+ data with both the MOD09 surface reflectance and MOD02 derived surface reflectance was performed in the RED, NIR, and SWIR bands (B3, B4, B5 for ETM+ and B1, B2, B6 for MODIS) to isolate the discrepancies that might be due to the differences in the atmospheric-correction processes used during spectral intercalibration of the MOD09 product and our ETM+ reflectance images.

MOD09GHK data were reprojected from the sinusoidal projection to the same Lambert Conformal Conic projection as the ETM+ images. The registration errors between MOD09GHK data and ETM+ ranged from 300 to 500 m based on visual assessments of ground control points identified in the ETM+ imagery.

Table 1. Characteristics of the Landsat-7 ETM+ scenes and the MODIS TOA radiances (MOD02GHK) and surface-reflectance (MOD09GHK) swaths used. The time acquisition corresponds to the scene or swath centre

Study area	Acquisition date	UTM raw/path	ETM+ scene center long./lat.	MODIS swath center long./lat.	ETM+ acquisition time (UTC)	MODIS acquisition time (UTC)	% Cloud in ETM+ scene	Land over date
MWP	05/07/2000	16/29	76.37° W 45.29° N	78.05° W 45.37° N	15:42	16:20	1.5	05/07/2000
AM	13/07/2000	08/29	64.25° W 44.60° N	63.83° W 45.30° N	14:52	15:30	10	13/09/1999
TS	20/08/2000	18/22	75.56° W 54.52° N	79.01° W 55.65° N	15:51	16:30	0.7	20/08/2000
BS	04/07/2000	25/26	88.91° W 48.86° N	92.32° W 45.46° N	16:36	17:15	0	04/07/2000

MWP – mixed wood plain, AM – Atlantic maritime, TS – taiga shield, BS– boreal shield.

Atmospheric correction of the MOD02HKM product was performed using the same processing chain applied previously to ETM+ data, but with MODIS-specific spectral settings in 6S, to result in a MOD02corr product. The LCC projection and subsetting of the MOD02HKM swath data were performed using the reprojection tool developed by Khlopenkov et al. (2006). The registration errors between MOD02HKM data and ETM+ were under 250 m based on comparison of 500 m MODIS bands with ETM+ imagery over ground control points.

All MODIS data were super-sampled to 30 m and cloud-contaminated areas were masked using the MODIS quality assurance data (QA) provided with the data products as well as areas mapped as cloudy in the Landsat land-cover maps.

MODIS and ETM+ intercalibration

Before proceeding to sensor intercalibration, there is a need to standardize the spatial scale of the surface-reflection data provided by MODIS and ETM+ scenes. The

Table 2. Land-cover classification legend based on CCRS FGDC classification, together with the Dominant Land-cover Group DLG stratification used for MODIS and ETM+ intercalibration.

	<i>Tree Dominated (tree-crown density > 25%)</i>
DLG1	1 Evergreen forest (>75% cover) — old
	2 Evergreen forest (>75% cover) — young
DLG2	3 Deciduous forest (>75% cover)
DLG3	4 Mixed coniferous (50–75% coniferous) — old
	5 Mixed coniferous (50–75% coniferous) — young
	6 Mixed deciduous (25–50% coniferous)
DLG1	7 Evergreen open canopy (40–60% cover) — moss–shrub understory
	8 Evergreen open canopy (40–60% cover) — lichen–shrub understory
	9 Evergreen open canopy (25–40% cover) — shrub–moss understory
	10 Evergreen open canopy (25–40% cover) — lichen (rock) understory
DLG2	11 Deciduous open canopy (25–60% cover)
	12 Deciduous open canopy–low regenerating to young broadleaf cover
DLG3	13 Mixed evergreen–deciduous open canopy (25–60% cover)
	14 Mixed deciduous (25–50% coniferous trees; 25–60% cover)
	15 Low regenerating to young mixed cover
DLG4	<i>Shrub dominated</i>
	16 Deciduous shrubland (> 75% cover)
	<i>Herb dominated</i>
	17 Grassland, prairie region
	18 Herb–shrub–bare cover, mostly after perturbations
	19 Shrubs–herb–lichen–bare
	20 Wetlands
	21 Sparse coniferous (density 10–25%), shrub–herb–lichens cover
	22 Sparse coniferous (density 10–25%), herb–shrub cover
	23 Herb–shrub
	24 Shrub–herb–lichen–bare
	25 Shrub–herb–lichen–water bodies
	26 Lichen–shrubs–herb, bare soil or rock outcrop
	27 Lichen–shrubs–herb, bare soil/rock outcrop, water bodies
	28 Low vegetation cover (bare soil, rock outcrop)
	29 Low vegetation cover, with snow
	30 Woodland–cropland
	31 Cropland–woodland
	32 Annual row-crop forbs and grasses — high biomass
	33 Annual row-crop forbs and grasses — medium biomass
	34 Annual row-crop forbs and grasses — low biomass
	35 Lichen barren
	36 Lichen–shrub–herb–bare
	37 Sparse coniferous (density 10–25%), lichens–shrub–herb cover
DLG5	<i>Vegetation not dominant</i>
	38 Rock outcrop, low vegetation cover
	39 Recent burns
	40 Mostly bare disturbed areas (e.g. cutovers)
	41 Low vegetation cover
	42 Urban and built-up
	43 Water bodies
	44 Mixes of water and land
	45 Snow/ice
	46 Clouds

MODIS point-spread function (PSF) (Huang et al. 2002) was applied to the ETM+ data. A 1.5 km rectangular moving window filter was applied to both ETM+ and MODIS imagery to reduce uncertainties due to geolocation error and differences in pixel footprint with view angle; although this latter effect is small within the overlap of the ETM+ and MODIS images.

In order to include the land-cover information in the intercalibration process, the four SILC land-cover maps were resampled from 30 m to 1.5 km. The FGDC land-cover classification was generalized with regards to the canopy structure by using five dominant land-cover groups (DLG): deciduous forest, conifer forest, mixed forest, shrub/herb/nonvascular-dominated canopies and nonvegetated areas (Table 2). DLG-specific regression fits were determined for MODIS and ETM+ vegetation indices (VIs) and surface reflectances in the RED, NIR, and SWIR bands. Theil–Sen regression (Fernandes and Leblanc, 2005) is applied since it accounts for measurement errors in both regressor and response variables and is unbiased in the presence of up to 29% outliers. In addition to the SR, ISR, and RSR indices, the intercalibration of MODIS and ETM+ was also investigated for NDVI.

Intercalibration performances were assessed by propagating VI errors to LAI errors. DLG-based VI–LAI empirical relationships developed in Canada Centre for Remote Sensing (CCRS) at Landsat spatial resolution (Fernandes et al., 2003) were applied to MODIS 500 m vegetation indices with and without intercalibration. The 30 m land cover based ETM+ LAI map was resampled to 500 m and used as reference LAI map. A direct comparison of LAI maps derived from intercalibrated MODIS VIs and the reference LAI map will result in residuals due to both VI intercalibration and land-cover scaling errors ('scaling + intercalibration' errors). The contribution of each of these two factors was isolated so the precision of only VIs intercalibration can be assessed.

RESULTS

Intercalibration with MOD02HKM to ETM+ versus MOD09GHK to ETM+

Figure 1 shows surface-reflectance intercalibration results for two of the study areas using MOD09 and MOD02corr data for DLG3 (mixed forest). Both MOD09 and MOD02corr show a similar trend of higher surface reflectance compared to ETM+ in the RED and SWIR bands, and a somewhat smaller but still positive bias in the NIR band. The biases for NIR and SWIR bands were relatively consistent between sensors across study areas and DLGs (not shown). Larger biases were noticed in the RED band when comparing ETM+ and MOD09 versus ETM+ and MOD02corr. The large bias in MOD09 versus ETM+ spectral intercalibrations could be due to differences in atmospheric correction. The ETM+ atmospheric correction used scene

averaged MODIS-based AOD, and water vapour and ozone concentrations over clear sky areas while MODIS products use values at each pixel location (Vermote et al., 2002). Secondly, the implementation of 6S applied is different from the MODIS implementation both in handling of adjacency and bidirectional reflectance distribution function (BRDF) effects and possibly in the specification of the aerosol model (Vermote et al., 1997). This highlights the need to apply identical data-processing chains to arrive at surface reflectances used during intercalibration. In light of this finding, we continue our discussion only with reference to the intercalibration using the MOD02-corr products atmospherically corrected in an identical manner to the ETM+ data.

Reflectances and vegetation indices intercalibration

Absolute (relative) surface-reflectance biases over all DLGs and all study areas ranged between 0.0064 (15%) and 0.016 (95%) in the RED, 0.007 (3%) and 0.021 (8%) in the NIR, and 0.037 (25%) and 0.046 (37%) in the SWIR. The highest biases correspond to the AM study area, and might be due to the presence of haze or shadowing not screened by cloud mask, resulting in excess of the robust regression tolerance to outliers. Over all the dominant land-cover group and study areas, the absolute (relative) vegetation index bias between MOD02corr and ETM+ ranges between -0.027 (3%) and -0.072 (8%) for NDVI, -0.65 (10%) and -24.7 (57%) for SR, -0.20 (17%) and -0.63 (25%) for ISR, and -0.57 (18%) and -13.89 (57%) for RSR. Figure 2 shows an example of the general trend of VIs intercalibration observed in each of the study areas together with surface reflectances. All of the VIs tested are proportional to NIR reflectances and decrease in proportion to SWIR and/or RED reflectances. Hence, the consistent underestimation in VIs shown by MODIS is a direct result of the large biases between reflectance bands in SWIR and RED in comparison to biases in NIR.

Effect of Land cover on ETM+ and MODIS intercalibration

The results in the previous section indicate that relatively unbiased spectral intercalibration of reflectances or VIs is possible on a study-area basis if the land cover is well known. For convenience we will term intercalibration results using local DLG-specific regressions the baseline case. However, in many cases land cover is not known *a priori* and, in any event, at moderate resolution (>250 m) there is evidence to suggest that pure land-cover classes are common (Latifovic and Olthof, 2004). The same type of relationships as those previously obtained in the baseline case were fitted when performing the intercalibration without DLG specification. A systematic underestimation of ETM+ data by MODIS was identified over all sites with bias values ranging from -0.03 (4%) to -0.06 (9%) for NDVI, -0.3 (24%) to -0.55 (30%) for ISR, -1.47 (19%) to -11.78 (47%) for SR and from -0.94

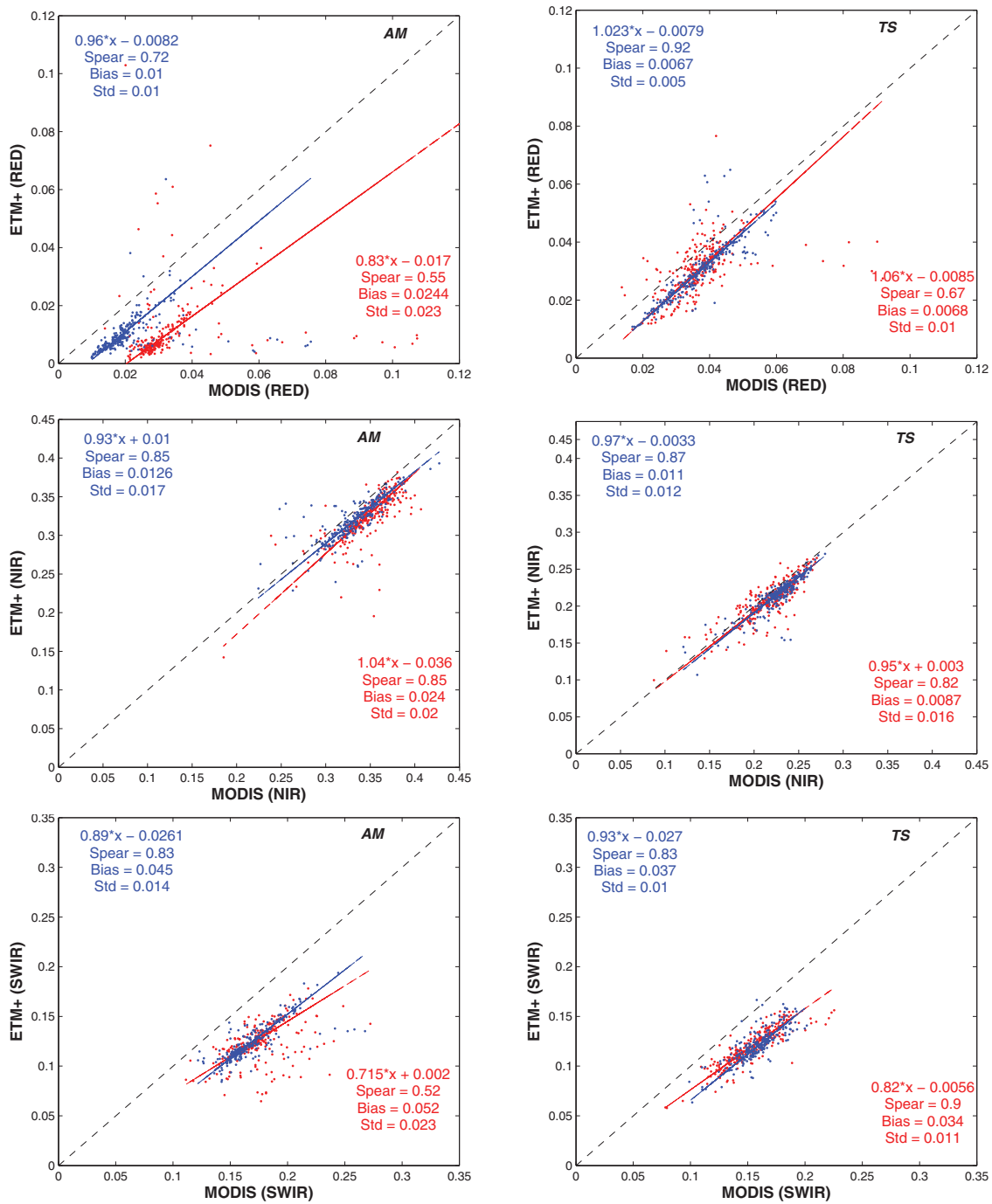


Figure 1. Spectral intercalibration of ETM+ and MODIS TOC reflectances based on dominant land-cover group and region-specific linear regressions using MOD09 (red) products and MOD02 radiance products (blue) for DLG3 (mixed forest) and Atlantic maritime (AM) and taiga shield (TS) study areas. The bias, Spearman's correlation coefficient (Spear), and standard deviation (Std) are provided.

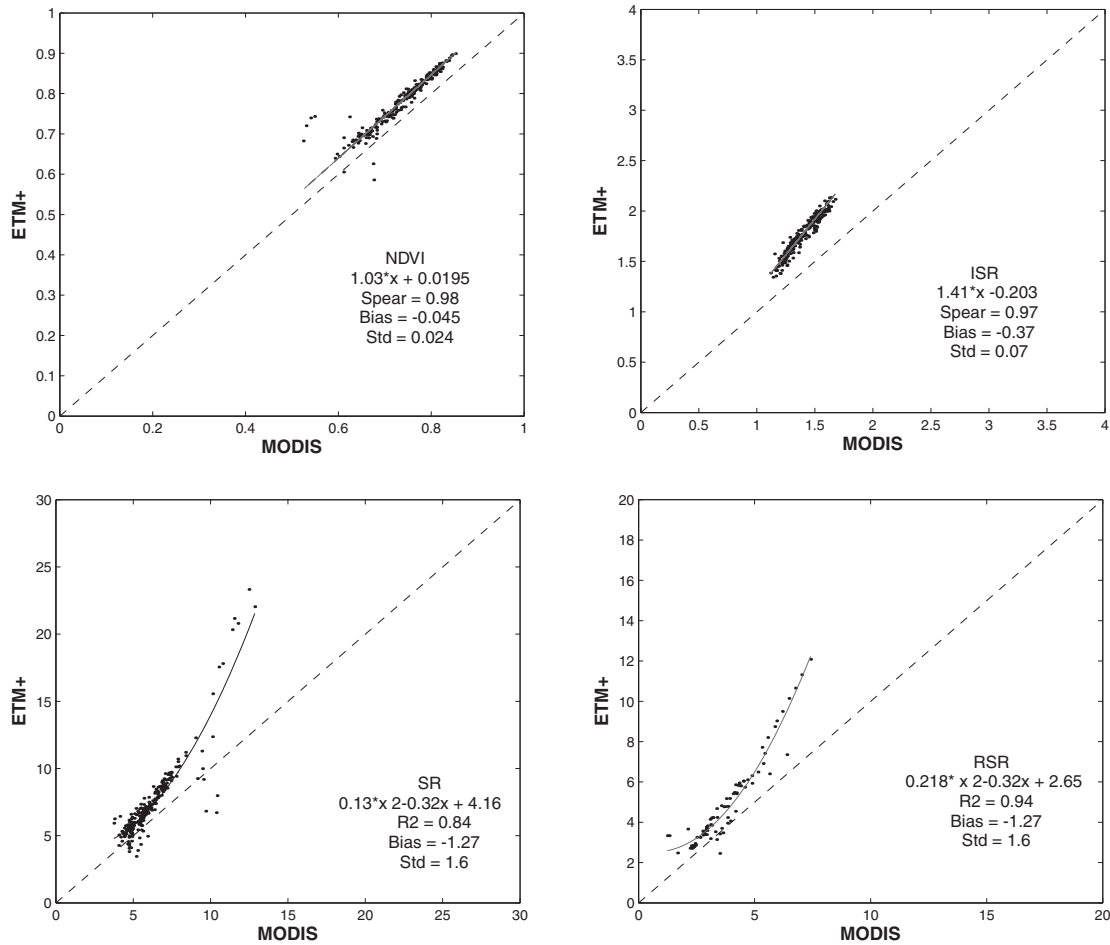


Figure 2. Intercalibration of ETM+ and MODIS TOC vegetation indices without specifying DLGs using MOD02 radiance products over the taiga shield (TS) study area. The bias, Spearman's correlation coefficient (Spear), and standard deviation (Std) are provided.

(22%) to –8 (51%) for RSR. Figure 3 summarizes the change in relative error in intercalibration, compared to the baseline case, over each land-cover groups and study area when performing site-specific intercalibration with no regard to the land-cover groups. Positive values mean that intercalibration has larger errors than the baseline case while negative values indicate the opposite. In the RED band, the BS and TS study areas show very low differences in errors (absolute values <3%) for all the land-cover groups while for MWP and AM study areas, the relative error increases by up to 7% for certain DLGs. In the NIR band, land cover seems to have a minimum effect on the sensor intercalibration for all the study areas with absolute value increases less than 1.1%. As for the SWIR band, the absolute values increased less than 3.1%. In some areas (e.g. TS), a single intercalibration for all DLGs actually decreased relative errors by between 0.5% and 1% compared to DLG-specific intercalibration. These small decreases were actually due to the fact that these DLGs tended to exhibit somewhat clustered distributions of ETM+ versus MODIS reflectances, so that the linear regression slope tended to exhibit greater residuals at low values

where relative errors tend to be magnified. When investigating the effect of land cover on vegetation indices intercalibration, NDVI index showed the lowest increase in relative errors (<1.6%), followed by ISR (<2.5%), SR (<6%), and finally RSR (<14%). The high RSR uncertainties noticed may be explained by the accumulation of the uncertainties of the three bands involved in the definition of this VI. This suggests that VIs that show good local performance for retrieving parameters, such as LAI, may incur additional errors when scaling to moderate-resolution sensors where land cover is not easy to clearly define.

Regional effect on sensor intercalibration

Taken to an extreme, the sensitivity of intercalibration to land cover was extended to consider the possibility of a universal intercalibration for all of our study areas.

An example of the effect of the study-area location on additional relative errors versus the baseline case is shown in Figure 4 for two study areas. Positive values mean that

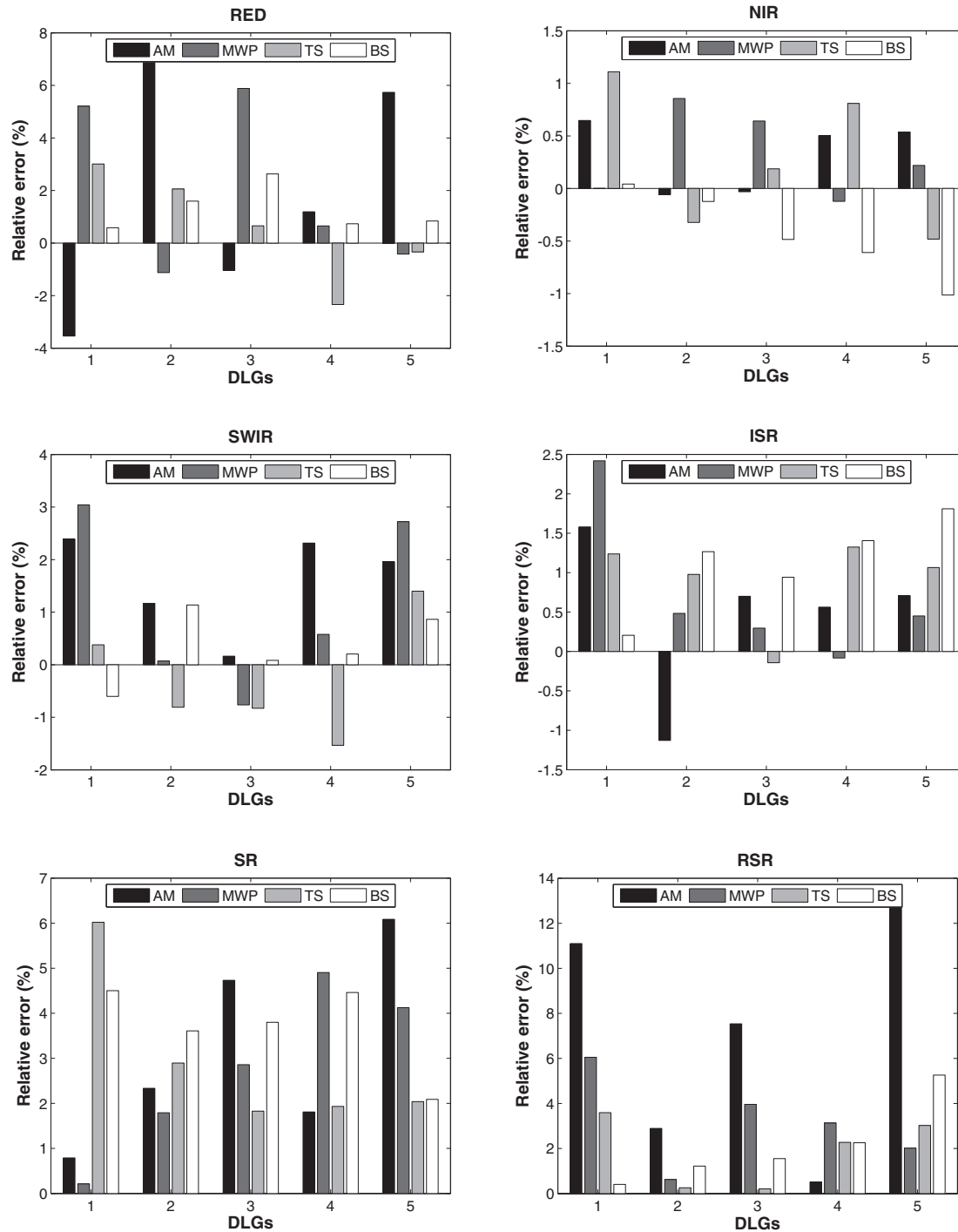


Figure 3. Change in the relative error between the baseline method and the intercalibration of ETM+ and MODIS based on one single regression across all DLGs. Relative errors are summarized for surface reflectances and vegetation indices by DLG type and study area. Positive values indicate lower uncertainties for the baseline method while negative values indicate the opposite. AM – Atlantic maritime, MWP – mixed wood plains, TS – taiga shield, BS – boreal shield.

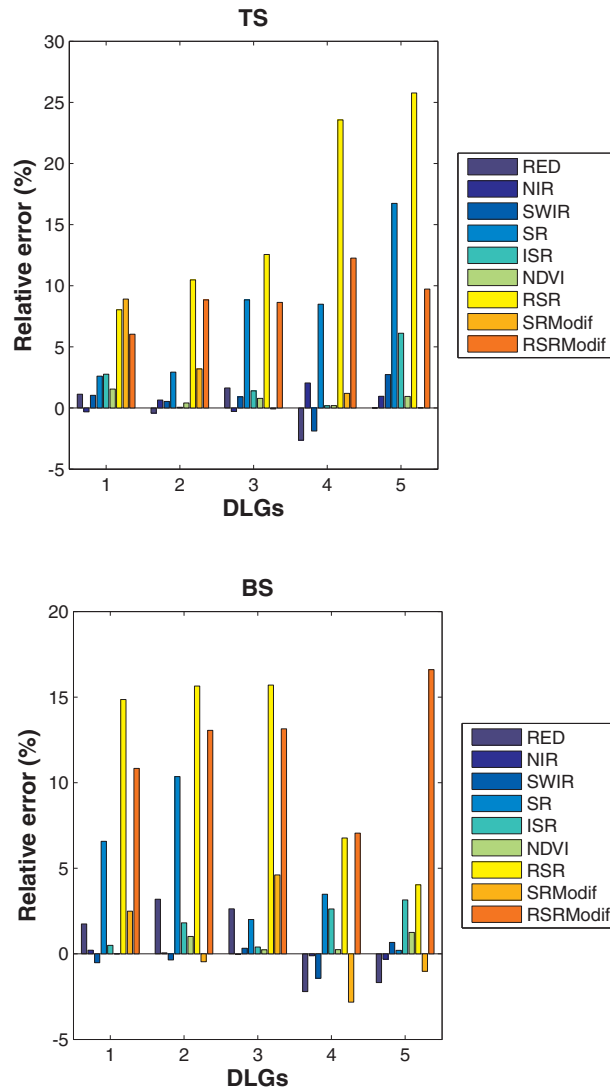


Figure 4. Change in the relative error between the baseline method and the intercalibration of ETM+ and MODIS based on one single regression across all DLGs and study areas. Relative errors are summarized for surface reflectances and vegetation indices by DLG type for taiga shield (TS) and boreal shield (BS) study areas. Please see text for abbreviations.

the baseline method has smaller errors than intercalibration without specifying area location, while negative values indicate the opposite. Ignoring the area location tends to globally increase intercalibration errors. The effect was generally low with regards to surface reflectance (absolute values <3%) except for the AM location in the red band, where additional relative error was about 13.5% due to the presence of haze and shadow in this scene. The NDVI and ISR vegetation indices showed low sensitivity to the study area location with absolute values generally lower than 3%. The sensitivity of SR and RSR VIs to the area location tended to be higher, ranging from 0.5% to 23% for SR and between 1% and 26% for RSR. Both the SR and RSR in the ETM+ data showed a range in values that exceeded the typical range used to derive

the LAI/VI transfer function from ground measurements (Fernandes et al., 2003, Stenberg et al., 2004). Therefore the effect of the area location was reassessed after setting the maximum VI to 15 for both SR and RSR. The best fits were achieved with linear regressions in this case. The results of these tests are labelled SR_Modif and RSR_Modif in Figure 4. In this case, data interpretation did not take into account the DLG1 and DLG3 in the AM study area due to lack of enough SR_Modif data to fit intercalibrations. A noticeable improvement was obtained, especially for SR index, with an increase in relative errors typically 5% except for MWP and TS study areas where it reached 7% for some DLGs. Although the RSR_Modif additional relative errors tend relatively to decrease, they are still significant with absolute values lower than 14%.

Assessment of sensor intercalibration for 500m LAI mapping

It is important to translate intercalibration errors into errors in parameter retrieval since the purpose of producing the VIs is ostensibly to relate them to land-surface parameters. In order to assess the effect of sensor intercalibration on LAI mapping, the prediction equations for LAI estimation from Landsat ETM+ provided in Fernandes et al. (2003) were applied in this study. The equivalent ETM+ NDVI, SR_Modif, and ISR were derived from MODIS data using the intercalibration formulas developed earlier. This investigation aims more to assess the consistency of 500 m LAI maps derived from ETM+ and MODIS data than the inherent accuracy of the LAI estimates. For this reason, all the areas labelled as crop (as opposed to grassland or pasture) were mapped using algorithms based on corn, the dominant crop in these regions, while mixed forest LAI was computed using the needle-leaf deciduous fraction map produced in CCRS at 1 km resolution (Pavlic et al., 2007). The ETM+ 30m LAI maps were resampled up 500 m and used as reference to evaluate the 500 m MODIS LAI maps.

Without intercalibration of VIs the MODIS LAI maps tends to underestimate the reference LAI with biases ranging from 0.73 to 2.61. Results (not shown) show that intercalibration errors are generally lower than 0.16 LAI unit. To put the intercalibration errors in context, land-cover scaling contributions are also investigated. When taking into account the scaling effect, differences between MODIS LAI and ETM+ LAI tend to increase substantially over all the study areas by more than 73% except for MWP study area where bias increase does not exceed 6%. Bias and median absolute error (MAE) values do not exceed 0.6 and 0.75 respectively. Some of these differences might be explained by the fact that in our study a 500 m MODIS pixel is considered as a single land-cover type which will be mapped by only one prediction equation, while the reference LAI is a sum of different LAI prediction equations weighted by the proportions of land-cover types present in the 500 m pixel.

The effect of land cover and study-area location on the VI intercalibration was also assessed over the LAI maps errors. Two additional LAI maps were derived for each study area using the ETM+/MODIS VI regressions previously developed without specifying the land-cover type or the site location. Neglecting the land-cover type or the site location globally tends to have a slight effect on the LAI biases (not shown).

CONCLUSION AND DISCUSSIONS

The effect of land-cover type on spectral intercalibration was very small in the NIR and SWIR bands. As for the RED, band errors were in some cases a little higher, up 7%, although some of this effect may be due to the presence of haze that varied between ETM+ and MODIS scenes. Similar results were observed when assessing the effect of study locations with even higher relative error in the RED. This implies that provided the clear sky conditions, intercalibration between ETM+ and MODIS would be independent of the land-cover type and the site location with less than 5% relative error. The effect of land-cover type and area location on spectral intercalibration of VIs varied with the type of VI considered. These intercalibrations were consistent over all the land-cover types and locations with relative errors lower than 3% for both ISR and NDVI. Increases in intercalibration error when ignoring land-cover type and area location tend to be higher for SR and RSR than observed for NDVI and ISR; especially for RSR where, for typical values ranges, absolute relative error can reach up 14%.

Our approach to intercalibration was able to quantify and correct for biases between sensors, but does not actually explain the cause of the observed differences. Uncertainties in radiometric calibration of one or both of MODIS on TERRA and ETM+ on Landsat 7 may explain these biases.

The impact of the vegetation indices' bias on LAI mapping depends on the type of VIs used. Without spectral intercalibration between MODIS and ETM+, the comparison of the reference ETM+ LAI to MODIS LAI maps derived using CCRS algorithms (ISR, SR, and NDVI) showed differences in LAI ranging between 0.73 and 2.61 LAI units. Land-cover scaling errors represents less than 26% in these differences. Application of ETM+/MODIS intercalibration to map leaf area index over the four areas showed that LAI can be derived from the calibrated MODIS VIs with less than 0.6 LAI unit uncertainties. Errors due to intercalibration do not exceed 0.16 LAI units. This work suggested that ETM+/MODIS VI intercalibration could be very useful to up-scale local LAI in situ data to generate regional LAI, especially in regions where errors associated to the MODIS LAI standard products are significant (Abuelgasim et al., 2006).

Leaf area index mapping approaches based on cross-sensor intercalibration should apply empirical bias correction that will need to be assessed at regional scales. Ideally, when mapping LAI by up-scaling method (Fernandes et al. 2003),

one should select VIs that do not suffer from bias effect provided that the relationship between LAI and VIs show similar performances.

Further studies with a wide range of acquisition geometry and sampling within the biomes we studied, and others, are recommended to assess both intercalibration and our method. In doing so this relatively straightforward approach for spectral intercalibration can be applied both for multiscale and multitemporal fusion of sensors to provide continuous information on land surface variables such as LAI.

REFERENCES

- Abuelgasim, A.A., Fernandes, R.A., and Leblanc, S.G., 2006. Evaluation of national and global LAI products derived from optical remote sensing instruments over Canada; *IEEE Transactions on Geoscience and Remote Sensing*, v. 44, no. 7, p. 1872–1884. doi:10.1109/TGRS.2006.874794
- Brown, M.E., Pinzon, J.E., Didan, K., Morisette, J.T., and Tucker, C.J., 2006. Evaluation of the consistency of long-term NDVI time series derived from AVHRR, SPOT-vegetation, SeaWiFS, MODIS, and Landsat ETM+ sensors; *IEEE Transactions on Geoscience and Remote Sensing*, v. 44, no. 7, p. 1787–1793. doi:10.1109/TGRS.2005.860205
- Cihlar, J., Guindon, B., Beaubien, J., Latifovic, R., Peddle, D., Wulder, M., Fernandes, R. and Kerr, J., 2003. From need to product: a methodology for completing a land cover map of Canada with Landsat data; *Canadian Journal of Remote Sensing*, v. 29, p. 171–186.
- Fernandes, R.A. and Leblanc, S.G., 2005. Appropriate linear regression techniques for the calibration of remote sensing models: when classical linear regression should not be used; *Remote Sensing of Environment*, v. 95, no. 3, p. 303–316. doi:10.1016/j.rse.2005.01.005
- Fernandes, R.A., Butson, C., Leblanc, S.G., and Latifovic, R., 2003. Landsat-5 and Landsat-7 ETM+ based accuracy assessment of leaf area index products for Canada derived from SPOT-4 VEGETATION data; *Canadian Journal of Remote Sensing*, v. 29, no. 2, p. 241–258.
- Galvao, L.S., Vitorello, I., and Filho, R.A., 1999. Effects of band positioning and bandwidth on NDVI measurements of tropical savannas; *Remote Sensing of Environment*, v. 67, p. 181–193. doi:10.1016/S0034-4257(98)00085-6
- Gao, X., Huete, A., Ni, W., and Miura, T., 2000. Optical–biophysical relationships of vegetation spectra without background contamination; *Remote Sensing of Environment*, v. 74, no. 3, p. 609–620. doi:10.1016/S0034-4257(00)00150-4
- Garrigues, S., Lacaze, R., Morisette, J., Baret, F., Weiss, M., Fernandes, F., Nickeson, J., Plummer, S., Yang, W., and Myneni R. 2006. Validation and intercomparison of global Leaf Area Index products derived from remote sensing data; *Journal of Geophysical Research*, v. 113, no. G02028. doi:10.1029/2007JG000635Huang, C., Townshend, J.R.G., Liang, S., Kalluri, S.N.V., and DeFries, R.S., 2002. Impact of sensor's point spread function on land cover characterization: assessment and deconvolution; *Remote Sensing of Environment*, v. 80, no. 2, p. 203–212. doi:10.1016/S0034-4257(01)00298-X

- Kaufman, Y.J. and Tanré, D., 1992. Atmospherically resistant vegetation index (ARVI) for EOS-MODIS; IEEE Transactions on Geoscience and Remote Sensing, v. 30, p. 261–270. doi:10.1109/36.134076
- Khlopenkov, K., Trishchenko, A.P., and Luo, Y., 2006. Novel method for reprojection of MODIS level 1B images based on concurrent gradient search; Proceedings of SPIE; Image and Signal Processing for Remote Sensing XII, v. 6365, p. 636 506.1–636 506.9.
- Latifovic, R. and Olthof, I., 2004. Accuracy assessment using sub-pixel fractional error matrices of global land cover products derived from satellite data; Remote Sensing of Environment, v. 90, no. 2, p. 153–165. doi:10.1016/j.rse.2003.11.016
- Liang, S., Fang, H., Chen, M., Shuey, C.J., Walthall, C., and Daughtry, C., 2002. Validating MODIS land surface reflectance and albedo products: Methods and preliminary results; Remote Sensing of Environment, vol. 83, p. 149–162.
- Miura, T., Huete, A. and Yoshioka, H., 2006. An empirical investigation of cross-sensor relationships of NDVI and red/near infrared reflectance using EO-1 Hyperion data; Remote Sensing of Environment, v. 100, p. 223–236. doi:10.1016/j.rse.2005.10.010
- Nemani, R., Pierce, L., Running, S., and Band, L., 1993. Forest ecosystem processes at the watershed scale: sensitivity to remotely-sensed leaf area index estimates; International Journal of Remote Sensing, v. 14, p. 2519–2534. doi:10.1080/01431169308904290
- Pavlic, G., Chen, W., Fernandes, R., Cihlar, J., Price, D., Latifovic, R., Fraser, R., and Leblanc, S.G., 2007. Canada-wide maps of dominant tree species from remotely sensed and ground data; Geocarto International, v. 22, no. 3, p. 185–204.
- Stenberg, P., Rautinien, M., Manninen, T., Voipio, P., and Smolander, H., 2004. Reduced simple ratio better than NDVI for estimating LAI in Finnish pine and spruce stands; Silva Fennica, v. 38, no. 1, p. 3–14.
- Teillet, P.M., Fedosejevs, G., Barker, J.L., Miskey, C.L., and Bannari, A., 2006. Spectral simulations of vegetation indices in the context of Landsat Data continuity; Proceedings of the International Geoscience and Remote Sensing Symposium (IGARSS06), Denver, Colorado, USA, p. 1784–1787.
- United States Geological Survey, 2004: Landsat-7 Science Data User's Handbook, United States Geological Survey, <<http://landsathandbook.gsfc.nasa.gov/handbook.html>> [accessed July 9, 2008].
- Venturini, V., Brisht, G., Islam, S., and Jian, L., 2004. Comparison of evaporative fractions estimated from AVHRR and MODIS sensors over South Florida; Remote Sensing of Environment, v. 93, no. 1-2, p. 77–86. doi:10.1016/j.rse.2004.06.020
- Vermote, E.F., El Saleous, N., Justice, C.O., Kaufman, Y.J., Privette, J.L., Remer, L.A., Roger, J.C., and Tanré, D., 1997. Atmospheric correction of visible to middle-infrared EOS-MODIS data over land surfaces: background, operational algorithm and validation; Journal of Geophysical Research, v. 102, p. 17131–17141. doi:10.1029/97JD00201
- Vermote, E.F., El Saleous, N.Z., and Justice, C.O., 2002. Atmospheric correction of MODIS data in the visible to middle infrared: first results; Remote Sensing of Environment, v. 83, no. 1-2, p. 97–111. doi:10.1016/S0034-4257(02)00089-5